Inhibition of Biofilm Growth on Highly Polycationic Polyelectrolyte Multilayers

by

Albert H. Park

SUBMITTED TO THE DEPARTMENT OF MATERIAL SCIENCE AND EDUCATION
IN PARTIAL FULFILLMENT OF THE REQUIREMENTS FOR THE DEGREE OF

BACHELOR OF SCIENCE
AT THE
MASSACHUSETTS INSTITUTE OF TECHNOLOGY

MAY 16, 2008
[June 2008]

Signature of Author: _____
Department of Material Science and Engineering
May 16, 2008

Certified by: _____
Michael F. Rubner
Professor of Material Science and Engineering
Thesis Supervisor

Certified by: _____
Caroline A. Ross
Professor of Material Science and Engineering
Chair, Undergraduate Committee

Inhibition of Biofilm Growth on Highly Polycationic Polyelectrolyte Multilayers

by

Albert H. Park

Submitted to the Department of Material Science and Engineering
on May 16, 2008 in Partial Fulfillment of the Requirements for the
Degree of Bachelor of Science in Material Science and Engineering

ABSTRACT

Research on the efficacy of antimicrobial polyelectrolyte multilayers (PEMs) in inhibiting S. epidermidis biofilm growth is presented here. Three known antibacterial PEM systems were used: poly(acrylic acid) (PAA)/ poly(allylamine hydrochloride) (PAH) assembled at pH 3.5/8.6, poly(sodium 4-styrene-sulfonate) (SPS)/PAH assembled at pH 9.3/9.3, and SPS/PAH assembled at pH 9.3/9.3 with acid treatment. The relative density of surface charges was measured via Rose Bengal staining and negatively-charged microsphere adsorption to correlate with biofilm growth and the polycationic biocidal effect. UV/visible microscopy was used to observe biofilm growth, and a rubric for categorization of biofilm growth patterns is proposed here. It was found that the number of biofilm formation sites decreased significantly when cultured on the PEMs used here.

Thesis Supervisors: Michael F. Rubner, TDK Professor of Polymer Materials Science and Engineering

TABLE OF CONTENTS

LIST OF FIGURES AND TABLES

ACKNOWLEDGEMENTS

First, I would like to thank my thesis advisors, Michael F. Rubner and Jenny A. Lichter. Much of the prior art in PEMs has been conducted in the Rubner lab, and the prior art for the anti-adhesion and antibacterial studies was primarily conducted by Jenny Lichter. Thank you to the MIT Department of Material Science and Engineering (DMSE), the Institute of Soldier Nanotechnologies (ISN), and the Boston University (BU) Department of Biomedical Engineering (BME) for allowing me use of their laboratory space and resources. Special thanks to Xin Brown at BU BME for guidance in the use of their quartz crystal microbalance with dissipation (QCM-D) and to Maricela Delgadillo for developing the static biofilm protocol used here. Also, thanks to the members of the Rubner group for their advice and company. These members include Gary Chia, Zek Gemici, Pinar Kurt, Koushik Mukherjee, Hiroomi Shimomura, Al Swiston, Wui Siew Tan, Soong Ho Um, and Erik Williamson.

Secondly, I would like to thank my friends and colleagues at MIT and around Boston who have made the last four years a worthwhile experience. Of distinction are Juan E. Prajogo, my crazy Finnish roommate of two years, Arthur T. Mak, my business partner for our last three ventures, and Karl Ruping, my mentor and boss at incTANK Ventures. Also, a shout-out to the Venerable Tenzin LS Priyadarshi for his meditations on the meaning of life, the members of the Chi Phi Fraternity for their gift of brotherhood, and my co-founders in Qfiniti LLC, Green Karma Technologies Inc., and Lobby 10 Consulting LLC for riding through the startup rollercoaster with me.

Finally, I would like to thank my parents Sung-Keun and Kyoung-Bog Park for enduring unimaginable difficulties and many sacrifices to raise my sister, Hyun-Joo (Julie) Park and me, Sang-Hoon (Albert) Park. Thank you to my father, Sung-Keun Park, for showing me the limitless potential of the human mind and the power of one's will. Thank you to my mother, Kyoung-Bog Park, for giving up her medical career to provide stability and support in my formative years. I wish you both an enlightened mind, free and re-opened to see truth in this world. Thank you to my older sister, Julie Park, whom I know little of but always find admiration in. May your extraordinary efforts lead you to a fascinating and fulfilling life. Also, thank you to all of my relatives in Korea for being there in my dreams. Apologies to my late grandfather, Ki-Joo Park, for not getting to know you. Also, apologies to my younger cousins for never being there for them as their eldest brother: Nam-Hoon, Yang-Hoon, Kwang-Hoon, Chi-Hoon, Chi-Soo, and my three other younger cousins whom I am very sorry to say I do not know the names of. *This thesis is dedicated to you.*

CHAPTER 1 INTRODUCTION

1.1 Introductory Remarks

Polyelectrolyte multilayers (PEMs) hold great potential in substrate and surface applications due to their highly engineerable and versatile characteristics. This chapter will cover the general mechanics of PEMs and their broad applications. First is an overview of the layer-by-layer (LBL) assembly method used to easily, cheaply, and safely create PEMs. Second is an exploration of the use of polyelectrolyte multilayers as antibacterial biomaterials. Thirdly is a review of biofilms. This chapter is concluded by a summary of this thesis' objectives and an outline. More in-depth introductions will also be provided with each chapter.

1.2 General Introduction

1.2.1 Layer-by-Layer polyelectrolyte multilayers

The layer-by-layer (LBL) assembly technique is an extremely versatile and easy to use technique to develop precisely controlled thin films for a broad range of applications, notably in biology and biomimetics. In LBL assembly, a charged solid substrate adsorbs layers of alternately charged thin film components in solution (depicted in Figure 1-1). In addition to electrostatic forces, newly adsorbed layers can be attracted by a range of forces, including hydrogen bonding and hydrophobic interactions.[10] In the case of the polyelectrolytes used in this research, all three PEM systems utilized electrostatic cross-linking to maintain structural stability. To increase PEM stability, thermal and photochemical treatment can be used to increase cross-

linking between layers or turn ionic linkages into covalent linkages. Upon adsorption of a new polyelectrolyte layer, the surface charge switches, and the oppositely charged polyelectrolyte is deposited. Two of these layers, which includes one negatively charge and one positively charged layer, is denoted as one bilayer.

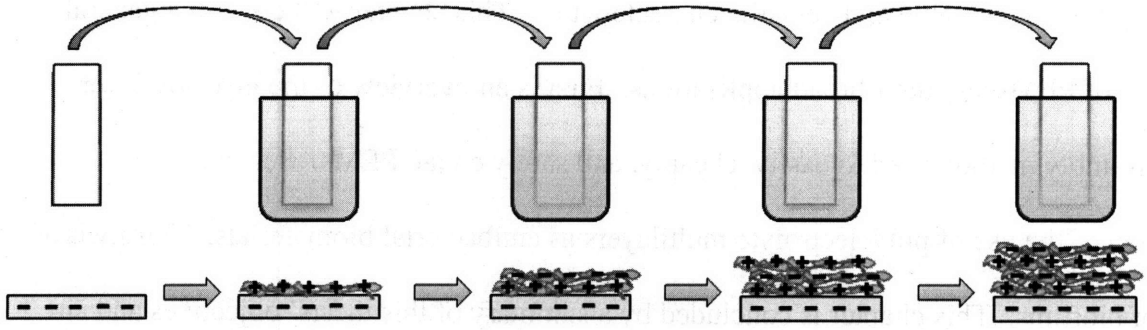

Figure 1-1. The layer-by-layer (LBL) adhesion process for polyelectrolyte multilayers (PEMs). A blank, charged substrate of either positive or negative charge (in this case, negative) is dipped in polyelectrolyte solutions of alternating charge to create electrostatic cross-linking across the layers. Not shown are water rinses between each dip that remove any loosely adhered polyelectrolyte.

Various properties of the PEMs can be finely tuned with the LBL process. pH adjustment of the polyelectrolyte dipping solutions enables control over conformation of polyelectrolyte chains by changing the degree of ionization, from long and rod-like to condensed and curly. This enables nanometer-scale control of layer and thin film thickness.[12] The surface charge can also be adjusted via pH to modulate the polyelectrolytes degree of ionization, and choice of a wide array of polyelectrolytes means a vast number of potential combinations. These PEMs can be built via LBL on a wide range of substrates, including glass, metals, polymers, nanoparticles, and nanowires. In addition, the LBL technique has been successfully demonstrated using dendrimers, proteins, DNA, and even viruses as the polyelectrolyte components.[10]

LBL assembly holds several key advantages over the older thin film Langmuir-Blodgett and self-assembled monolayer (SAM) thin film assembly techniques. The method, pioneered by Decher et al in 1992, is simpler, faster, and more stable than Langmuir-Blodgett deposition.[3] LBL films also have a higher loading capacity than SAMs due to their multiple layers. The aforementioned versatility of substrates and components is also a benefit of LBL over both Langmuir-Blodgett and SAMs.[10] Anti-cell adhesion and anti-microbial surfaces have also been constructed by grafting of polymer chains to a substrate. The resulting films are not as uniform in surface coverage and lack the nanoscale controllable thickness of LBL films.[11] Most LBL PEMs are assembled in water-based solutions, which is more environmentally sound. [12]

1.2.2 Antibacterial properties of polyelectrolyte multilayers

Polyelectrolyte multilayers have been functionalized to exhibit antibacterial properties through several methods. One of the first successful demonstrations utilized silver nanoparticles embedded within the polyelectrolyte multilayers.[9] A newer antibacterial mechanism of action involves functionalizing a surface with high density polycationic chains that provide a non-leaching, permanent biocidal effect. Significant work has been done with quaternary ammonium salts, N-alkyl-polyethylenimine, and quaternized poly(vinylpyridine), all of which exhibit antibacterial properties through the polycationic effect.[4,7,8]

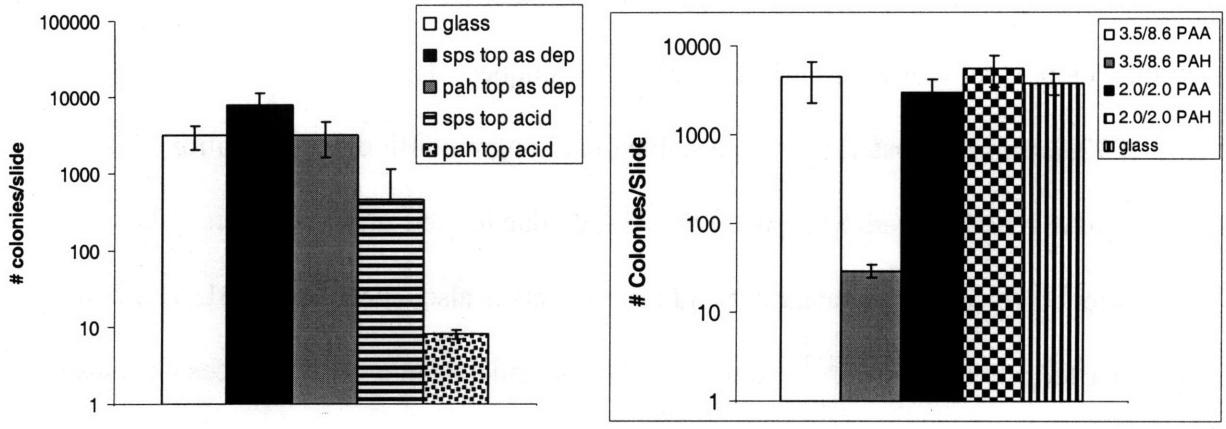

Figure 1-2. Antibacterial effects of the SPS/PAH (left) and PAA/PAH (right) systems.

Prior art has established two recurring theories on the exact polycationic antibacterial mechanism of action. The first mechanism is based on an ion exchange between the bacterial cell membrane and the functionalized polycationic surface. Bacterial cell membranes are stabilized by mobile, divalent cations such as Mg^{2+} and Na^{2+}. In Gram negative bacteria, these stabilizing cations hold together the opposing phosphate groups of the lipopolysaccharides in the outer cell membrane. When in close proximity to the positive charge from a polycationic surface, the divalent stabilizing cations migrate out of the membrane via an ion-exchange mechanism. This leads to a failure in the cell membrane integrity and, subsequently, cell death. (Figure 1-3) Gram positive bacteria have a different cell membrane structure, but they have also been shown to exhibit similar behavior.[4]

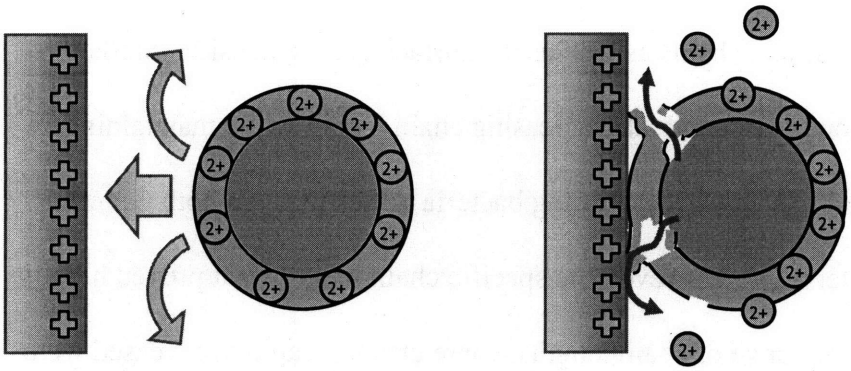

Figure 1-3. The theorized ion exchange that occurs between high density surface polycationic charges and mobile divalent cell membrane cations leads to cell death via membrane rupture.

In the second mechanism of action, hydrophobic chains ending with cationic charge penetrate the cell membranes, much as a needle would puncture a balloon. The positive charge attracts the negatively charged bacterial membrane, and the hydrophobic chain insinuates itself into the phospholipids bilayers, leading to cell leakage. (Figure 1-4) Given that the cell membrane thickness of Gram negative E. coli is approximately 46 nm and that the cell membrane thickness of Gram positive Bacillus subtilis is approximately 45-55 nm, a polycationic chain length of 75 nm would be required for full penetration.[7]

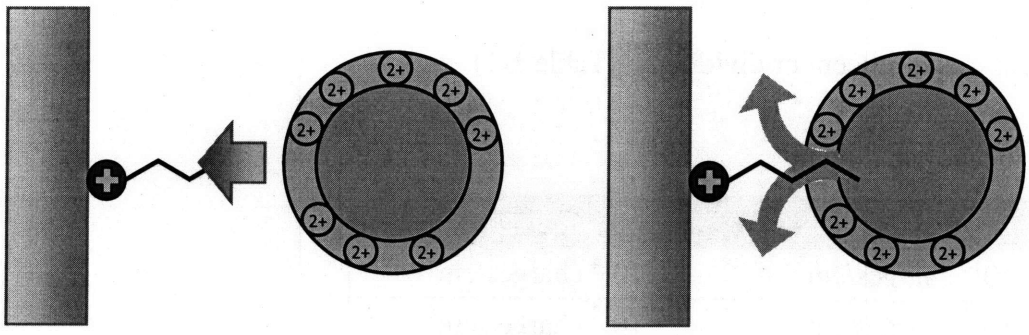

Figure 1-4. The membrane-piercing effect of hydrophobic, cationic chains that result in bacteria death via membrane rupture.

These two mechanisms have been investigated both alone and in combination by manipulating the chain length of surface polycationic chains as well as the surface charge density. Studies focusing on chain length variation have found that increasing chain length while maintaining constant cation charge density correlates with increasing bacteria kill efficacy in both Gram positive and Gram negative bacteria.[7,8] However, the specific chain lengths that proved highly effective in instant cell kill and the range of chain lengths where efficacy rapidly increased were below the theorized minimum chain length required to fully penetrate bacteria cell membranes. Furthermore, very short chain lengths (10 nm) relative to theorized minimum penetration length (75 nm) were shown to cause cell death.[7]

Studies restricting chain length and instead varying surface charge density also found a positive correlation between surface charge density and bacteria kill efficacy. These studies focused on the cationic charges found within the first nanometer of the charged surface. These are the only charges possibly felt by nearby bacteria based on the Debye-Hückel screening length of the surface cations.[7] This mechanism of action was found to have a threshold surface charge density that varied according to whether the bacteria was Gram positive or Gram negative and whether the bacteria was quiescent or dividing.[4] (Table 1-1)

	Gram positive	Gram negative
Quiescent	10^{14} charges/cm^2	10^{14} charges/cm^2
Dividing	10^{13} charges/cm^2	10^{12} charges/cm^2

Table 1-1. Threshold surface charge densities for optimal bacteria kill based on bacteria characteristics.[4]

Dividing cells required less surface charge density to kill, which Kügler et al explained by the fact that bacteria have more fragile, sensitive cell membranes during division.[4] When the

surface charge density was greater than $5x10^{15}$ charges per cm^2, cell contact-killing was achieved regardless of increased charge density or modification to chain length. Interestingly enough, Murata et al pointed out that the surface charge of E. coli is $5x10^{14}$ to $5x10^{15}$ charges per cm^2.[7] Live/dead two-color fluorescence stains in studies of both mechanisms of action have shown the bacterial cause of death to be cell membrane rupture.[4, 8]

1.2.3 Bacterial Biofilms

Biofilms are tenacious superstructures of one or more bacterial and/or fungal species colonized in an exopolysaccharide matrix. These superstructures even have nutrient channels and differentiated cells, similar to the tissues of more complex organisms. Biofilms are found in both natural and industrial environments with substrates prone to bacterial adhesion. Examples include sewage pipes, dead tissue, medical devices, and other such inert, wet surfaces.[2] The mechanics of biofilm growth and differentiated bacteria cell behavior enable them to withstand harsh environments, immune-system responses, and antibiotics. These inherent properties make biofilms the cause of 65% of all nosocomial infections and $1 billion annually in health treatment costs in the United States alone.[1,5]

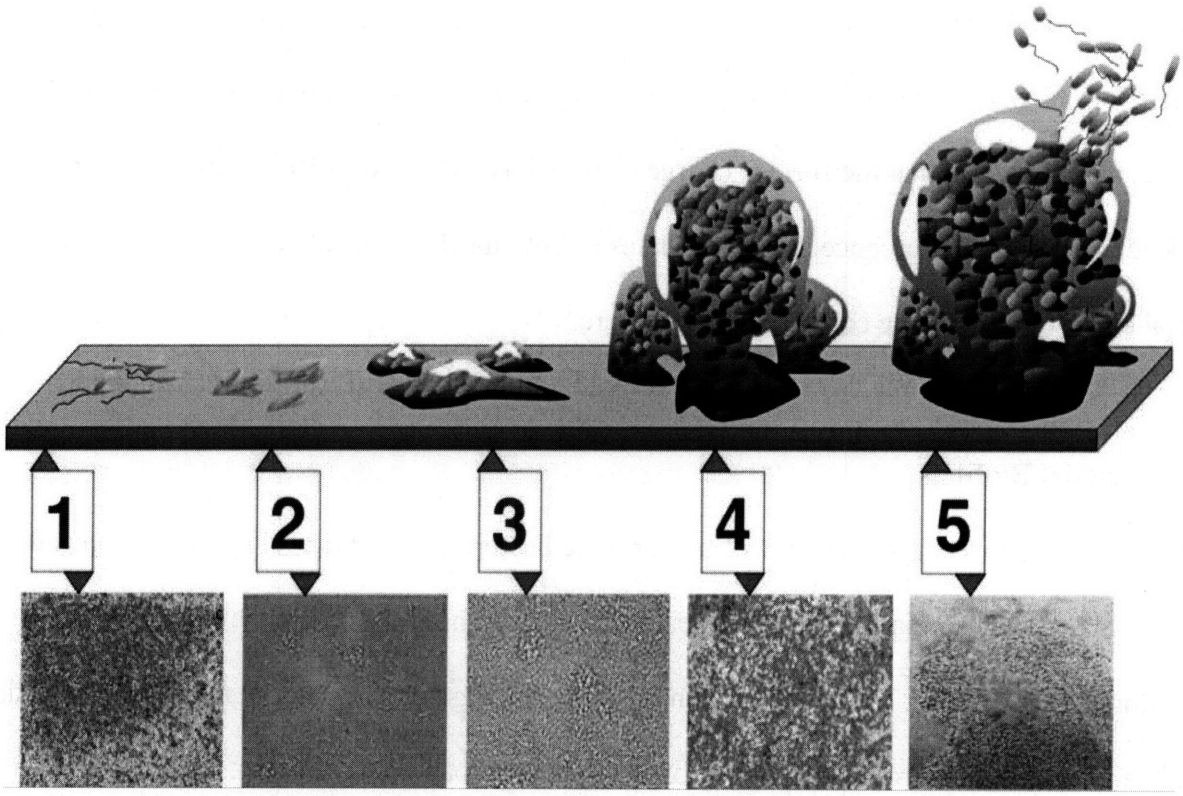

Figure 1-5. Stages of biofilm growth (from left to right): initial attachment, irreversible attachment, maturation I, maturation II, dispersion. Associated photomicrographs are of P. aeruginosa biofilms.[6]

Bacteria in biofilms can become ten to one thousand times more resistant to antimicrobial agents versus when they exist in primitive colonies. This resistance is theorized to rise from three primary contributors. The first is the failure of antimicrobial agents to penetrate the biofilm. The exopolysaccharide matrix that is characteristic of all biofilms presents an initial barrier to diffusion of antimicrobial agents into the biofilm. The second is the prevalence of slow-growth cells from nutrient limitation in mature biofilms. These slow-growth cells become less susceptible to antibiotics. Thirdly, heterogeneity, or differentiation of bacteria, within biofilms creates varying susceptibility to antimicrobial agents. Bacteria within different regions of the biofilm play varying roles depending on their immediate environments, resulting in expression of biofilm-specific phenotypes that can be more resistant to biocidal treatments.[5]

1.3 Thesis Objectives and Outline

This research aims to advance knowledge of the cationic antibacterial mechanism of action by: 1) isolating the non-penetration mechanism of action with weak and strong PEMs and correlating to PEM free surface cation density, and 2) testing efficacy of the non-penetration mechanism of action in inhibiting growth of Gram positive S. epidermidis bacteria biofilms.

The first objective of mechanism of action characterization was pursued through quantification of free amine group density on the surface of poly(allylamine hydrochloride) (PAH) topped PEMs via negatively charged stains and microparticles. The second objective to test biofilm inhibition was tested with static growth of a biofilm-forming strain of S. epidermidis on sample PEMs.

REFERENCES FOR CHAPTER 1

[1] Costerson, J.W.; Lewandowski, Z.; Caldwell, D.E.; Korber, D.R.; Lappin-Scott, H.M. *Annual Rev Microbiol* **1995**, 49, 711.

[2] Costerson, J.W.; Stewart, P.S.; Greenberg, E.P. *Science* **1999**, 284, 1318.

[3] Decher, G.; Hong, J.D.; Schmitt, J. *Thin Solid Films* **1992**, 210, 831.

[4] Kügler, R.; Bouloussa, O.; Rondelez, F. *Microbiology* **2005**, 151, 1341.

[5] Mah, T.C.; O'Toole, G.A. *Trends in Microbiology* **2001**, 9, 34.

[6] Monroe, D. *Public Library of Science Biology* **2007**, 5, e307.

[7] Murata, H.; Koepsel, R.R.; Matyjaszewski, K.; Russell, A.J. *Biomaterials* **2007**, 28, 4870.

[8] Park, D.; Wang, J.; Klibanov, A. *Biotechnology Progress* **2006**, 22, 584.

[9] Shi, Z.; Neoh, K.G.; Zhong, S.P.; Yung, L.Y.L.; Kang, E.T.; Wang, W. *Journal of Biomedical Materials Research Part A* **2005**, 76A, 826.

[10] Tang, Z.; Wang, Y.; Podsiadlo, P.; Kotov, N.A. *Advanced Materials* **2006**, 18, 3203.

[11] Yang, S.Y.; Mendelsohn, J.D.; Rubner, M.F. *Biomacromolecules* **2003**, 4, 987.

[12] Yoo, D.; Shiratori, S.S.; Rubner, M.F. *Macromolecules* **1998**, 31, 4309.

CHAPTER 2 CONSTRUCTION OF POLYELECTROLYTE MULTILAYERS

2.1 Introduction

Three polyelectrolytes were used in this research: poly(allylamine hydrochloride) (PAH), poly(acrylic acid) (PAA), and poly(sodium 4-styrene-sulfonate) (SPS) (Figure 2-1). The use of two anionic polyelectrolytes allowed for the comparison of both weak and strong PEMs. Here, the weak and strong refer to the ability to change the degree of disassociation, or ionization, of the tested polyelectrolyte groups with pH.

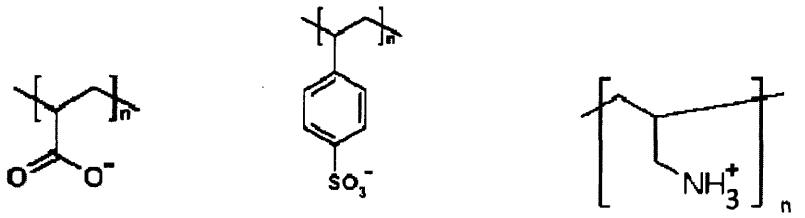

Figure 2-1. Structures of the polyelectrolytes used in this research (from left to right): PAA, SPS, PAH

The bilayers of both polyanion/polycation combinations are held together via electrostatic cross-links without any further treatment. The stability of PEMs can be increased through thermal and photochemical cross-linking to withstand physiological and even harsh conditions.[6] The systems tested were PAA/PAH assembled at pH 3.5 (PAA) and 8.6 (PAH) and SPS/PAH assembled at pH 9.3 (SPS and PAH). Given that PAH was the cation source in all tested systems, PAH was always the surface layer. A third system was added by acid treating the SPS/PAH 9.3/9.3 system after construction. These specific systems were chosen for their promising antibacterial activity seen in bacterial cell adhesion tests conducted with non-biofilm forming S. epidermidis. From a molecular perspective, it makes sense to explore these three

systems due to the high prevalence of free positive amine groups in the PAH surface layer of all three PEM systems.

2.2 Experimental Methods

2.2.1 PEM construction

Materials. Poly(acrylic acid) (MW = 90 000, 25% aqueous solution) (PAA) was obtained from Polysciences. Poly(allylamine hydrochloride) (MW = 70 000) and poly(sodium 4-styrene-sulfonate) (MW = 70 000) were obtained from Aldrich. All polyelectrolytes were used without further purification. All polyelectrolyte solutions used were 10^{-2} M based on repeat unit molecular weight. Solutions and water rinses were made with 18 MΩ MilliQ water. The PEM substrates used were standard glass microscope slides from VWR, aminosilane functionalized glass slides from Sigma, polystyrene petri dishes and 6-well tissue culture plates from BD Falcon, and SiO_2 coated quartz crystal microbalance sensors (QSX 303) from Q-Sense.

Dipping Procedures. The PAA/PAH system was built on a silane-functionalized glass microscope slide with 6 bilayers for surface charge measurements. The silane-functionalized surface changes the glass substrate's charge from negative to positive. This substrate was used for previous experiments with the PAA/PAH system, and kept in this experiment to maintain validity in data comparisons from prior art. For biofilm growth substrates, PAA/PAH PEMs were built on standard, negatively charged, polystyrene petri dishes with 5.5 bilayers. SPS/PAH non-treated and acid-treated PEMs were built on negatively charged glass microscope slides with 15.5 bilayers for surface charge measurements. The same two systems were also built on

negatively charged polystyrene six-well tissue culture plates with 15.5 bilayers. All PEMs were built to present the polycation, PAH, on top, and the particular numbers of bilayers were chosen to avoid substrate effects.

PEMs were built on a Carl Zeiss HMS Series Programmable Slide Stainer. PEMs were dipped in pH-adjusted polyelectrolyte solutions for 15 minutes, followed by two agitated 2-minute water rinses and one agitated 1-minute water rinse after each polyelectrolyte dip to remove loosely adhered polyelectrolytes. The pH's used in the PAA/PAH system were pH 3.5 for PAA and 8.6 for PAH. The pH's for both the SPS/PAH untreated and acid-treated systems were pH 9.3 for SPS and 9.3 for PAH. The water rinses for the SPS/PAH systems were adjusted to pH 9-10 to prevent changes in ionization between polyelectrolyte dips. All pH's were adjusted with HCl or NaOH only, with no mixing of the two to minimize solution salt concentration.

QCM-D PEM growth. A Q-Sense E4 quartz crystal microbalance with dissipation (QCM-D) was used to demonstrate PEM growth atop the SiO_2 substrate of the QCM-D sensors. 10^{-2} M polyelectrolyte solutions of polyacrylamide (PAAm) at pH 3.0 and PAA at pH 3.0 with pH 3.0 water rinses were used as in the dipping procedure. Each polyelectrolyte was flowed through the QCM-D chamber at a flow rate of 0.1 mL per minute until frequency measurements decreased and leveled off (10-15 minutes), indicating completed adhesion of a new layer. This was followed by a water rinse until the frequency no longer changed, indicating removal of all loosely adhered polyelectrolyte. Adhesion and rinse was then repeated with the complement polyelectrolyte to complete a bilayer. PAA/PAH and SPS/PAH PEMs on QCM-D sensors were built with the automated dipping procedure using a customized Teflon sensor holder for faster

and easier production of PEM coatings. The negatively charged SiO_2 substrate was compatible with the protocol used with negative glass microscope slides as the substrate. The only change in protocol was the addition of a plasma cleaner step to clean QCM-D sensors prior to dipping.

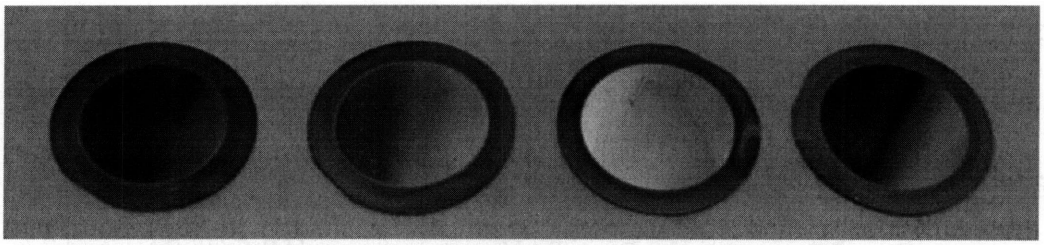

Figure 2-2. A full set of QCM-D sensors ready for biofilm growth. From left to right: PAA/PAH 3.5/8.6, SPS/PAH 9.3/9.3 untreated, SPS/PAH 9.3/9.3 acid-treated, blank SiO_2 substrate.

2.2.1.1 pH Control of PEM growth

The thickness of adsorbed polyelectrolyte layers can be finely controlled on a nanometer level through adjustments in polyelectrolyte solution pH. The amount of polyelectrolyte adsorbed is determined by the surface charge density of the underlying layer. This surface charge density is derived from the linear charge density and conformation of the polyelectrolyte chains. Both factors are controlled by pH, which controls the degree of ionization of polyelectrolyte chains. Highly ionized side groups will oppose each other, leading to a stretched out, rod-like conformation of the polyelectrolyte chains (Figure 2-3). The new surface effectively masks all electrostatic forces of the underlying layer, resulting in surface charge being solely dependent on the top-most layer.[7] Thus, by adjusting pH of polyelectrolyte solutions relative to polyelectrolyte pK_a, thickness of the successive layers can be finely tuned. In the PEM systems, SPS, with a solution pK_a of 1-2, was almost 100% ionized in solution given a pH of 9.3 and pK_a of 1-2. PAA was >50% ionized in solution with a pH of 3.5 and pK_a of 4-5.[4] PAH has a solution pK_a of 8-9 and was used at both pH 9.3 and 8.6.[1]

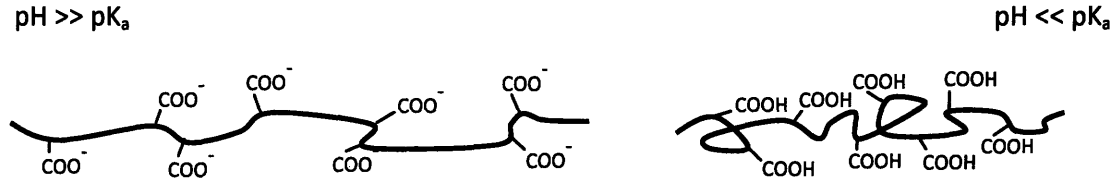

Figure 2-3. The effect of pH on conformation and linear charge density in PAA

The weak PAA/PAH system allows for greater control of PEM thickness via pH modulation versus the strong SPS/PAH system. The degree of ionization of weak polyelectrolytes is very sensitize to variation from the pK_a, and as a result has a greater range of ionization versus strong polyelectrolytes.

2.2.2 Acid treatment of SPS/PAH PEMs

The SPS/PAH acid-treated samples were immersed in a pH 2.5 aqueous solution for 15 minutes, followed by a one minute rinse in neutral DI H_2O and drying with compressed air. Prior to acid treatment, assembly pH of the SPS/PAH system resulted in completely ionized, stretched-out adsorbed SPS chains and partially ionized, coiled/looped adsorbed PAH chains. The low linear charge density of the hydrophobic PAH caused the highly coiled, energetically favored conformation which electrostatically bonded to SPS at ionized sites. During acid treatment at pH 2.5, the degree of ionization of PAH increases from 70% after pH 9.3/93 assembly to over 95%. The linear charge density of PAH increases due to the increase in degree of ionization and shifts the conformation-dominating force from hydrophobic association to electrostatic repulsion. Figure 2-4 illustrates the resulting change in conformation, which has been measured using in situ AFM as a consistent order of magnitude increase in RMS roughness.[2] This balance of electrostatic opposition and hydrophobic association has been unequivocally demonstrated in

similar SPS/PAH PEMs built above pH 8.5 where low pH post-treatment caused swelling and subsequent high pH post-treatment caused shrinking. The swelling thickness was 400-500% dry thickness.[1, 2]

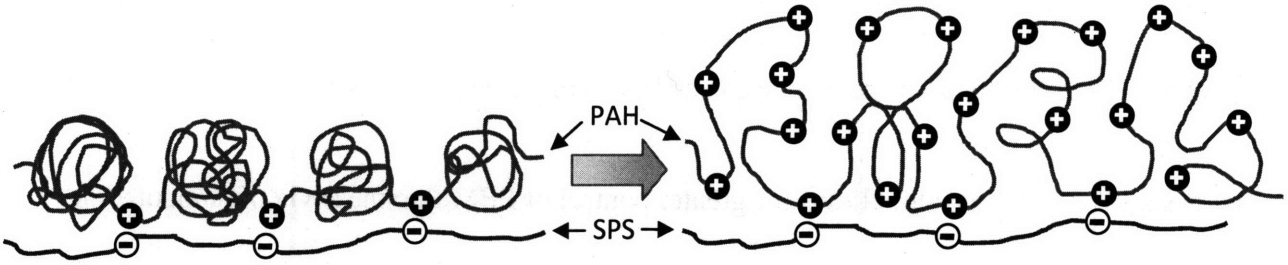

Figure 2-4. The effect of acid-treatment on the bilayers of pH 9.3/9.3 SPS/PAH PEMs. The untreated PEM is on the left, and the acid treated PEM is on the right.

2.3 Results and Discussion

The PEM growth protocols adapted from previous experiments with the PAA/PAH and SPS/PAH systems worked without any difficulties. Given the flexibility of the LBL assembly method, swapping glass substrates for polystyrene and SiO_2 did not cause any problems. There is a minor concern relating to the substrate geometry of the 6-well polystyrene tissue culture plates. The surrounding walls and relatively small surface area of the well bottoms may cause decreased reliability in PEM uniformity. Thickness measurements of produced PEMs on these substrates calculated via ellipsometry can solve this concern. Growth of PEMs via QCM-D proved successful, but the time-intensive process and limited batch size (maximum of 4 sensors at a time) made it impractical for repeated PEM growth. As a result, all QCM-D sensor PEMs were assembled using the automated dipping protocol.

The assembly and acid treatment pH's for all samples were determined from prior art, and did not require further experimentation. Antimicrobial properties, anti-adhesion properties, swellability, and acid treatment of relevant PEMs had already been characterized and fairly well understood.

2.4 Conclusion

PAA/PAH and SPS/PAH PEMs can be easily and reliably produced using automated dipping procedures on glass and SiO_2 substrates. The LBL process has proved to be useful in PEM construction for the given weak and strong polyelectrolyte systems where pH served as the main variable.

REFERENCES FOR CHAPTER 2

[1] Hiller, J. Rubner, M.F. *Macromolecules* **2003**, 36, 4078.

[2] Itano, K.; Choi, J.; Rubner, M.F. *Macromolecules* **2005**, 38, 3450.

[3] Notley, S.M.; Eriksson, M.; Wågber, L. *Journal of Colloid and Interface Science* **2005**, 292, 29.

[4] Shi, X.; Shen, M.; Möhwald, H. *Progress in Polymer Science* **2004**, 29, 987.

[5] Shiratori, S.S.; Rubner, M.F. *Macromolecules* **2000**, 33, 4213.

[6] Yang, S.Y.; Mendelsohn, J.D.; Rubner, M.F. *Biomacromolecules* **2003**, 4, 987.

[7] Yoo, D.; Shiratori, S.S.; Rubner, M.F. *Macromolecules* **1998**, 31, 4309.

CHAPTER 3 SURFACE CHARGE CHARACTERIZATION

3.1 Introduction

In order to effectively examine the high density polycationic antibacterial mechanism, the surface charge density of utilized PEMs must be quantified. One of the primary mechanisms of action proposed for this biocidal effect is a positively-charged surface that induces an ion screening effect whereupon mobile, divalent stabilizing cations in the bacteria cell membrane migrate out via ion exchange. This leads to a failure in the membrane's structural integrity, and thus, cell death. To further investigate this mechanism of action, various methods were used to quantify the surface charge of the SPS/PAH and PAA/PAH PEM systems. Dansyl Chloride (5-(dimethylamino)naphthalene-1-sulfonyl chloride) molecules selectively react with the primary amino groups found in PAH, and fluoresces at DAPI wavelengths after reacting. These molecules are commonly used as a tagging reagent in protein sequencing and amino acid analysis. Rose Bengal (4,5,6,7-tetrachloro-2',4',5',7'-tetraiodofluorescein) is a negatively charged molecule used to stain sample PEMs in the visible spectrum, with characteristic absorption maxima at 525nm and 565nm.[1]

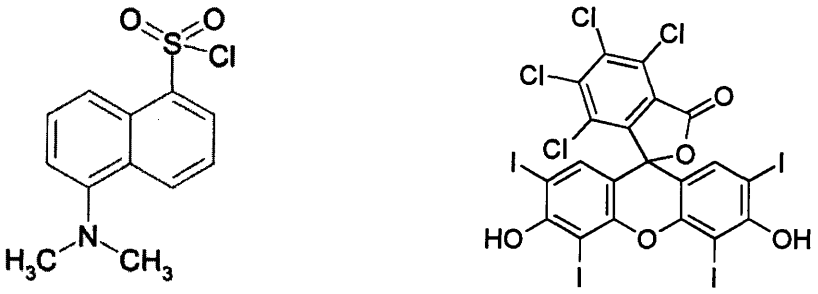

Figure 3-1. The molecular structures of negatively charged stains Dansyl Chloride (left) and Rose Bengal (right).

Charged melanin resin and latex microspheres were also used to measure charge and adhesion to the PEM surface. Microparticles have the benefit over dyes in only adhering to sample surfaces in contrast to the dyes which are also absorbed in the PEM bulk. Analysis of the resulting data could further characterize the antibacterial behavior and validate the aforementioned kill mechanism.

3.2 Experimental Methods

The following methods all reflect the density of free amines on the surface of the PAH topped PEMs. In this case, the term 'surface charge density' refers to the density of positive free surface amines, not the general positive charge of the PAH layer. The latter is correlated to the linear charge density of the polyelectrolyte and its conformation, and was not be measured by the following amine-binding methods.

Materials. Dansyl Chloride (5-(dimethylamino)naphthalene-1-sulfonyl chloride) was obtained from Calbiochem. Rose Bengal (4,5,6,7-tetrachloro-2',4',5',7'-tetraiodofluorescein) was obtained from Aldrich. (Figure 3-1) Carboxylate-modified, FITC-modified microparticles of melanin resin (D = 1.0 μm, 2.5% solid suspension) were obtained from Sigma Aldrich. Amine-functionalized latex microspheres (D = 1.0 μm, 2.63% solid suspension) were purchased from Polysciences. All water used in solutions and rinses was 18 MΩ MilliQ water. All surface-modified samples were imaged with a Zeiss Axioplan 2 UV/visible microscope using Axiovision image acquisition software. Stained samples were measured using a Cary 500i UV-Vis-NIR

Spectrophotometer to acquire absorbance spectra. Zeta potential measurements were carried out with a Zeta PALS by Brookhaven Instruments.

Dansyl Chloride stain. Dansyl Chloride is highly insoluble, and requires sufficient dimethylformamide (DMF) to stay in solution. The staining protocol was adopted from a previous protocol developed by Michael Berg in the Rubner Lab and from a protein tagging protocol released by Invitrogen Therapeutics. A 0.01 M and 0.05 M stock solution of Dansyl Chloride is first made in DMF. This stock solution is then stirred vigorously into a 0.1-0.2 M buffer solution of sodium bicarbonate ($NaHCO_3$) at pH 9 at a ratio of 1 mL stock solution to 10 mL buffer. The resulting mixture is sonicated to ensure thorough mixing and dissolution. Sample PEMs are then agitated in the Dansyl Chloride stain solution for 2, 5, and 15 minutes. Stained PEMs are blow dried and stored in vacuum if not being immediately used. Imaging was conducted via fluorescence microscopy with a DAPI filter.

Rose Bengal stain. Rose Bengal (4,5,6,7-tetrachloro-2',4',5',7'-tetraiodofluorescein) was chosen as an alternate negatively-charged stain, and has the disadvantage of not being specifically reactive to primary amines like Dansyl Chloride. 10^{-3} M solutions of Rose Bengal at pH 5 were used to stain PEM samples at time lengths of 1, 5, 10, 30, and 60 minutes. After sitting in Rose Bengal solution, stained PEMs were rinsed with pH 4-5 DI water and blow dried. Variation in the amount of absorbed stain could be seen visibly and with absorbance spectra measured via spectrophotometry.

Negatively charged microparticle adhesion. Amino- and carboxyl- functionalized microspheres approximately 1.0 μm diameter were used to measure both surface charge and adhesion characteristics of PEMs. A 1:1000 volume ratio of amino-functionalized microspheres in DI water was used to create a dipping solution for PEM samples. The solution pH was 5.66, and was sonicated to break up any microsphere clusters. PEMs were submerged in the microparticle suspension for 10 minutes before removing and blow drying. The density of amino-functionalized microspheres was measured through imaging with visible microscopy at 50x magnification. The same 1:1000 volume ratio of negatively charged microspheres and DI water was used to create a pH 6.6, 10 minute dip for PEM samples. The carboxyl-functionalized microparticles were modified with a fluorescent tag, which allowed them to be viewed through fluorescence microscopy with a FITC filter. 50x magnification images were used to measure microsphere surface density. To measure the actual microparticle charges, PEMs were built on the microparticles and zeta potential measurements were taken before each new layer. The zeta potential measurements, which represent the electrokinetic potential of particulates, found that the amino-functionalized were actually negatively charged instead of positively charge for some unknown reason. As such, all amino-functionalized microsphere data was not included here. The carboxyl-functionalized microparticles were negatively charged, as expected.

3.3 Results and Discussion

Dansyl Chloride staining failed to produce significant fluorescence to allow for accurate absorbance spectra. Dansyl chloride stock solution concentration was increased from 0.01 M to 0.05 M Dansyl Chloride in DMF, but resulted in the precipitation of Dansyl Chloride out of

solution upon mixing the stock solution and buffer. As a result, Rose Bengal was pursued as an alternate method. Rose Bengal proved much more effective in measuring surface charge, and significant variation was measured in stain adsorption among the different samples. The SPS/PAH acid treated system was the most darkly stained, followed by the SPS/PAH untreated and PAA/PAH systems. (Figure 3-2)

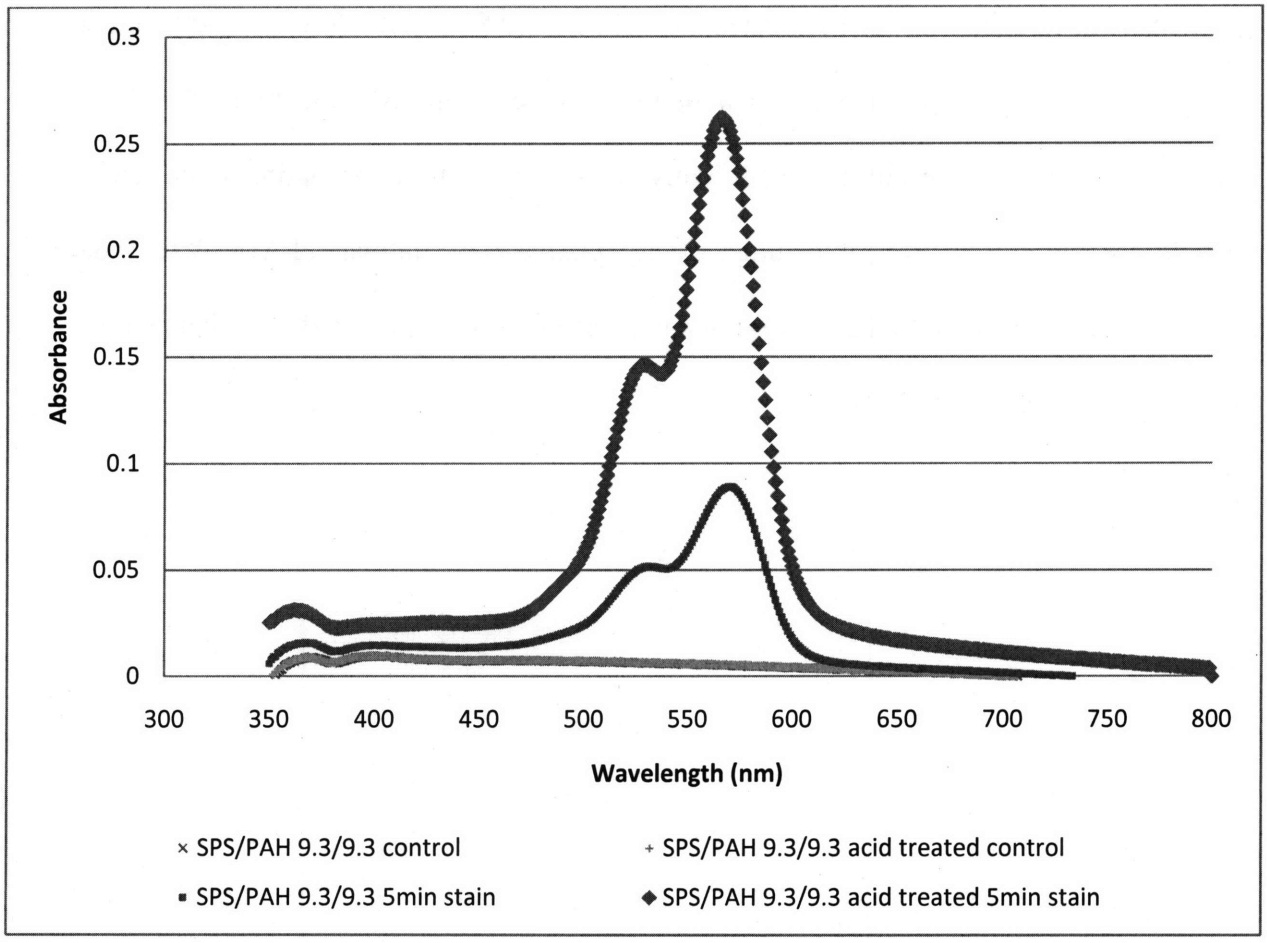

Figure 3-2. Absorbance spectra of untreated and acid-treated SPS/PAH PEMs before and after 5 minute Rose Bengal stains. Rose Bengal's characteristic absorbance peaks can be seen around 525 nm and 565 nm.

Special care must be taken to ensure that the Rose Bengal stain primarily adheres to the surface, versus absorbance through the volume. To minimize absorbance, staining duration was varied

from 1 to 60 minutes. The resulting absorbance spectra were used to identify ideal staining time lengths under the threshold absorbance. The results for the SPS/PAH acid system, seen in Figure 3-3, show that adsorption of Rose Bengal continues in the PEM even after 60 minutes. The SPS/PAH untreated system, however, quickly reaches a saturation point. This can be seen in the negligible increase in absorption spectra between the 5 minute stain and the 60 minute stain. (Figure 3-4) This staining behavior can be explained by the significant structural and electrostatic differences between untreated and acid-treated SPS/PAH PEMs. Acid treatment increases PAH's degree of ionization, making more amine groups available to bond with negative Rose Bengal molecules. This is likely the primary factor contributing to the acid-treated PAH's high Rose Bengal loading capacity relative to the untreated PAH. A secondary factor that may contribute to the absorption rate is the 400-500% swelling that occurs with hydrated acid-treated SPS/PAH.[1]

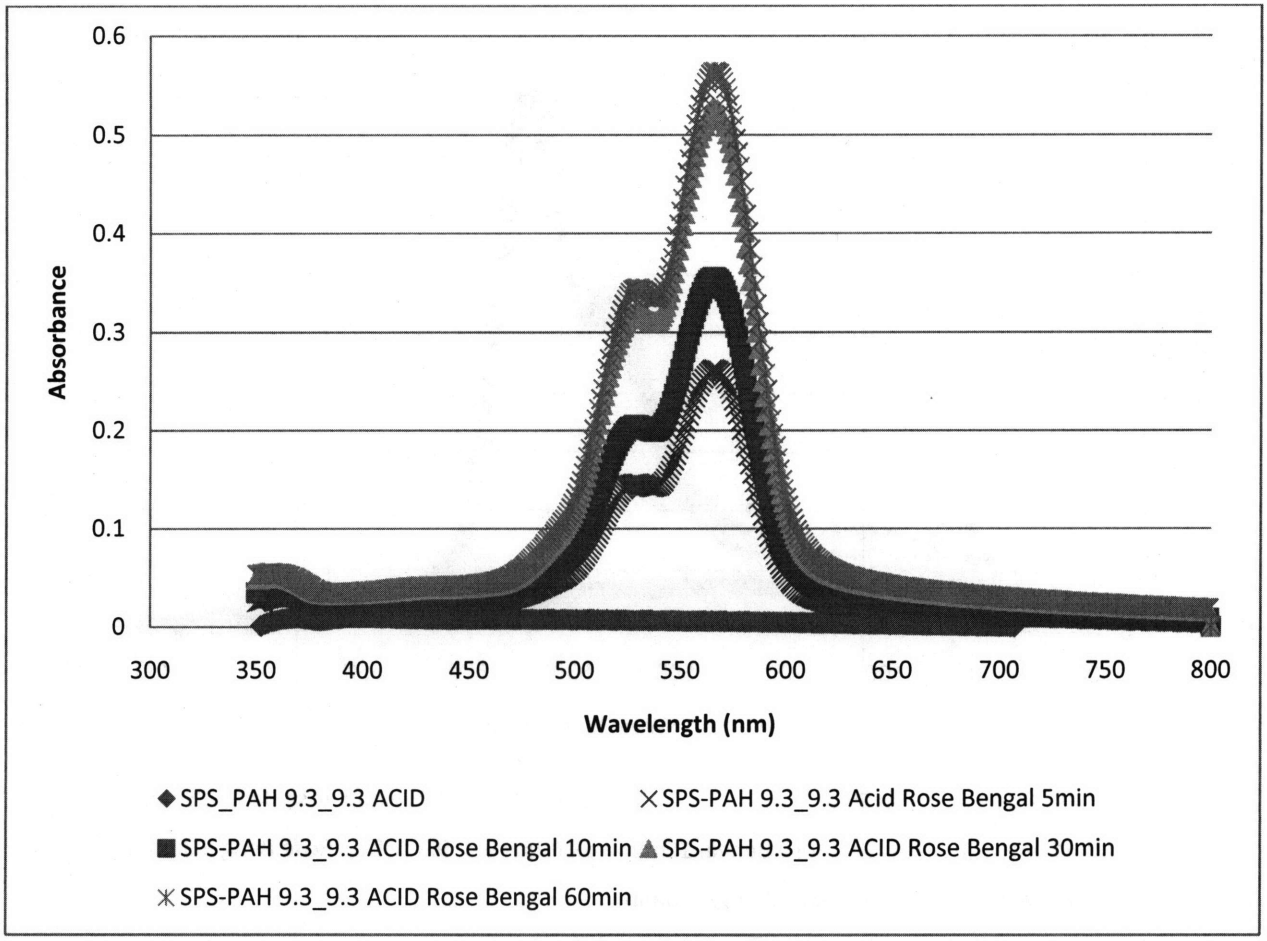

Figure 3-3. The absorbance spectra of acid-treated SPS/PAH PEMs after varying Rose Bengal stain time lengths.

The SPS/PAH acid treated system continually absorbs Rose Bengal dye up to one hour. At this point, it can be presumed that Rose Bengal is absorbing into the PEM bulk, which is much larger than the untreated SPS/PAH, and bonding to irrelevant free amines underneath the surface.

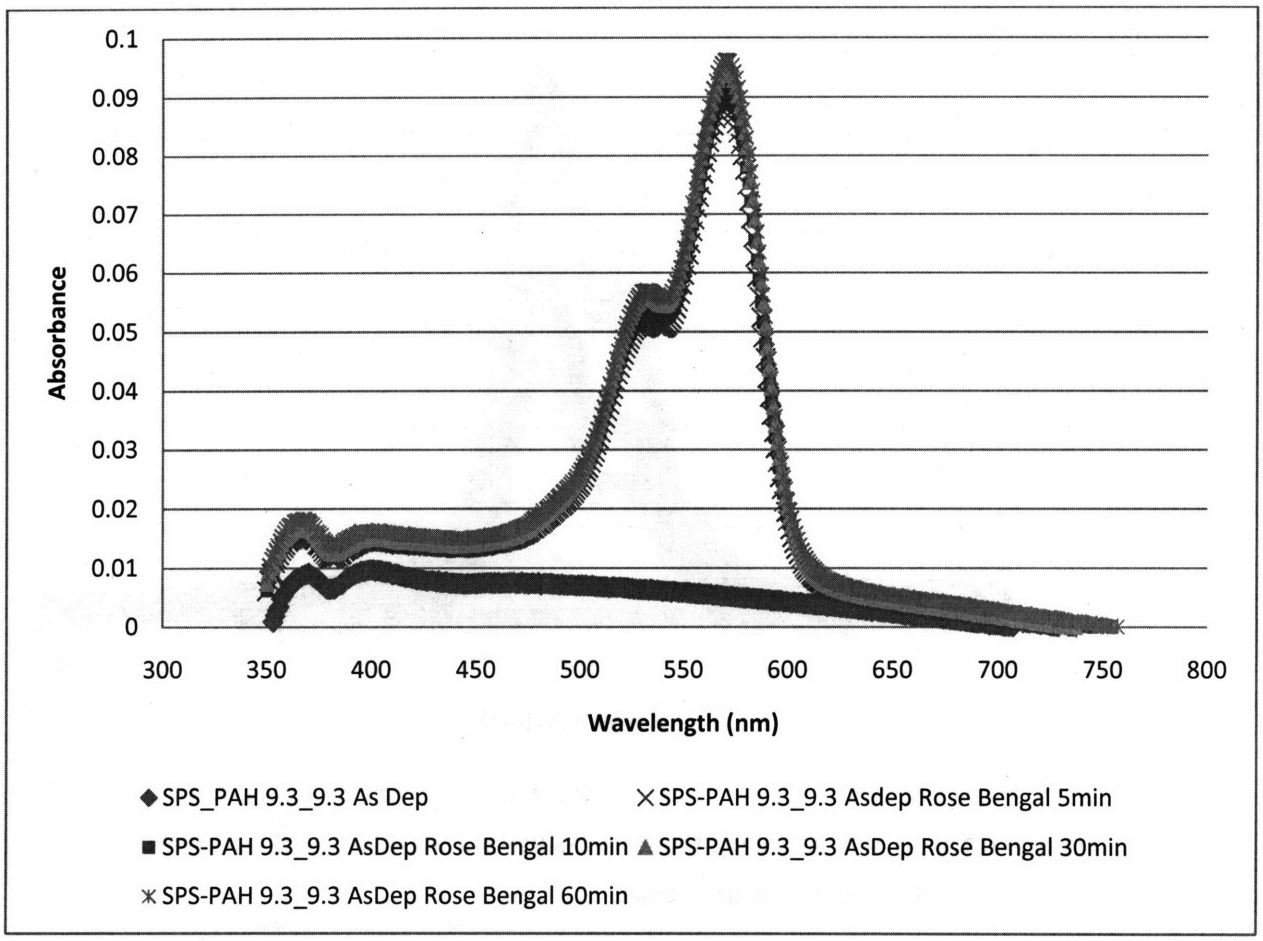

Figure 3-4. The absorbance spectra of untreated SPS/PAH PEMs treated with varying Rose Bengal stain time lengths.

In contrast to the acid-treated SPS/PAH system, the untreated PEM reached Rose Bengal saturation after just five minutes of staining, which was the shortest time tested. This rapid time to saturation can be explained by the fact that Rose Bengal has fewer free amines to bind to and less bulk to travel through. Another difference is the amount of Rose Bengal absorbed, which is much less than in the SPS/PAH acid treated system. After 5 minutes of staining, the acid-treated system already has an absorption maxima three times larger than the untreated system. This difference in Rose Bengal uptake rate means that equal stain lengths will result in absorption spectra that reflect different PEM depths of penetration. The absorption spectra for the 5 minute stains are the ideal data set to use, given that shorter staining times will decrease the difference in

staining depth. To accurately model the surface charge felt by bacteria near the PEM surface, it is important to ensure that surface charge measurements only take into account free amines located within an order of 1 nm from the surface, which is the approximate Debye-Hückel screening length of the PAH cations.[4] Otherwise, cationic charges within the PEM bulk will provide false contributions to the calculated surface charge. There is also the remote possibility that this as-deposited SPS/PAH system is very slow in absorbing Rose Bengal. This can be confirmed with even longer stain time lengths, but given the absorbance data at five, ten, thirty, and sixty minutes, this behavior is highly unlikely.

Given that zeta potential measurements revealed that the amino-functionalized microparticles were negatively charged, all related data was excluded from analysis. The carboxyl-modified microparticles were correctly charged, and were imaged successfully via fluorescence microscopy with a FITC filter. (Figure 3-5)

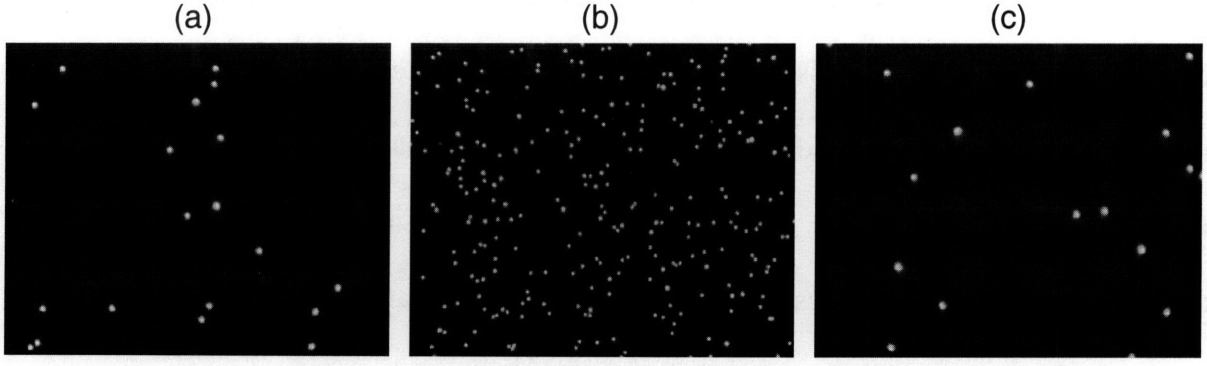

Figure 3-5. Adhesion of negatively charged 1.0 μm melanin resin microspheres on the surface of PAH-topped PEMs. (a) PAA/PAH, (b) SPS/PAH untreated, (c) SPS/PAH acid-treated. All images taken at 50x magnification.

The microparticle adhesion data reveals some interesting insights on surface activity due to two contributing factors affecting the microparticle density. The first is the surface and near-surface density (< 1 nm depth) of cation charges on PAH. The untreated SPS/PAH system seen in

Figure 3-5(b) clearly shows more adsorbed microparticles compared to the untreated PAA/PAH system in Figure 3-5(a). This difference can be explained by the use of a weak polyanion in PAA/PAH versus a strong polyanion in SPS/PAH, which results in different swelling properties and surface charges. In addition, the PAA/PAH system may have more amine groups paired to carboxylic acid groups at the surface because the PAH was adsorbed at a lower pH (8.6) than in the SPS/PAH (pH 9.3).

	PAA/PAH 3.5/8.6	SPS/PAH 9.3/9.3 untreated	SPS/PAH 9.3/9.3 acid treated
Average microparticle count	11.0 ± 5.7	248.4 ± 30.0	11.4 ± 4.2

Table 3-1. Average number of negatively charged microparticles adhered to PEM surfaces.

The second factor varying surface microparticle density is the structure and mechanics of the PEM bulk. The acid-treated SPS/PAH system forms a hydrogel structure which has been shown to exhibit anti-adhesion properties.[2,3] From a molecular perspective, the expanded PEM hydrogel illustrated in Figure 2-4 is composed of around 75% water by volume. [5] This results in a lack of a stable substrate for adhesion and a decrease in the magnitude of surface energy minimization that favors adhesion. Data comparing the untreated and acid-treated SPS/PAH systems support the expected adhesion behavior, with the acid treated surface showing a microparticle density an order of magnitude less than the untreated surface.

Another possible mechanism that has not been extensively pursued is the fact that expanded PAH surface chains from acid treatment have a very high kinetic energy at room temperature. The vibration and movement of these surface chains may physically shake away adhering

microparticles, in addition to contributing to the unstable hydrogel interface. The increase in RMS roughness seen in acid-treated vs. untreated SPS/PAH PEMs suggests that the height of these PAH chains may be at least 20 nm to 70 nm tall.[2] In situ height AFM measurements would give better estimate of chain/cluster height and surface morphology.

3.4 Conclusion

Dansyl Chloride staining and amino-functionalized microsphere adhesion proved ineffective in providing accurate data on the density of surface cations in the model systems. Rose Bengal staining found that acid-treated SPS/PAH had greater surface charge density than untreated SPS/PAH, which was expected. Furthermore, negatively-charged microparticle adhesion showed conclusive data that untreated SPS/PAH has a greater surface charge density than PAA/PAH. Thus, acid-treated SPS/PAH has the greatest surface charge density and PAA/PAH has the least amongst the three PEM systems. The acquired data is not yet sufficient for quantified surface charge density calculations, given the unknown depth of Rose Bengal absorption into the bulk of measured SPS/PAH samples.

REFERENCES FOR CHAPTER 3

[1] Hiller, J. Rubner, M.F. *Macromolecules* **2003**, 36, 4078.

[2] Itano, K.; Choi, J.; Rubner, M.F. *Macromolecules* **2005**, 38, 3450.

[3] Mendelsohn, J.D.; Yang, S.Y.; Hiller, J.A.; Hochbaum, A.I.; Rubner, M.F. *Biomacromolecules* **2003**, 4, 96.

[4] Murata, H.; Koepsel, R.R.; Matyjaszewski, K.; Russell, A.J. *Biomaterials* **2007**, 28, 4870.

[5] Yang, S.Y.; Mendelsohn, J.D.; Rubner, M.F. *Biomacromolecules* **2003**, 4, 987.

CHAPTER 4 STATIC BIOFILM GROWTH

4.1 Introduction

Biofilms are sophisticated colonies of one or more bacteria and/or fungi with primitive nutrient channels, differentiated phenotype expression, and an exopolysaccharide structure. These structures are able to withstand antibiotic treatments and harsh environments, and are a major source of recurring infections. In this research, the antibacterial and anti-adhesion properties of the PAA/PAH and SPS/PAH PEM systems are tested against biofilm growth. If such an approach is effective, then there is potential in use of such polycationic coatings as a prophylactic surface treatment to inhibit biofilm growth.

4.2 Experimental Methods

Materials. Biofilm forming S. epidermidis (ATCC 35984) was obtained from the ATCC. Soy trypticase broth was used as the bacterial growth medium.

S. epidermidis culture growth. Live S. epidermidis (ATCC 35984) was scraped off from a frozen pellet and resuspended in approximately 40 mL of sterile soy trypticase broth. The suspension was placed in a 37°C incubator on a shaker for 18 hours, or until cloudy. Bacteria cell density was then measured via absorbance spectrophotometry and diluted with soy trypticase broth to a density of 10^8 cells per mL.

Growth on polystyrene. 2-4 mL of the S. epidermidis suspension was pipetted into sterile polystyrene petri dishes and six well tissue culture plates with PAA/PAH, SPS/PAH untreated, SPS/PAH acid-treated, and blank polystyrene substrates. These biofilm assays were placed in an incubator at 37°C for 2 hours to allow for bacterial adhesion and initial biofilm growth. After the growth period, the bacterial suspension was very carefully pipetted out and the remaining biofilms were rinsed twice with phosphate buffered saline (PBS) before fixing with methanol for 20 minutes. Once the methanol was pipetted out and biofilm dried, the biofilm samples were stained with crystal violet. Visible and fluorescence microscopy were used to image stained biofilm structures.

QCM-D Protocol. Q-Sense E4 QCM-D flow chambers were first sterilized by running 10 mL of 70% ethanol through each flow chamber loaded with a PEM-coated sensor, then rinsed with 20 mL of 18 MΩ MilliQ water in each chamber at a rate of 0.88 mL per minute. The 10^8 bacteria/mL suspension in soy trypticase broth was flowed through each chamber at 0.1 mL per minute and then stopped for 2 hours. Sterile soy trypticase broth followed at the same flow rate for the next 12 hours, or overnight, to support biofilm growth. Chambers were heated to 37°C during the adhesion and growth periods.

4.3 Results and Discussion

4.3.1 Biofilm imaging

Images taken via fluorescence microscopy with a FITC filter showed high contrast images of the biofilms, which appeared red, on the substrates, which appeared green. Establishing

characteristic traits in biofilm growth for each sample system was difficult given the widely varied patterns of biofilm growth seen within each substrate. Overall, four general patterns of biofilm growth were observed. Seen in Figure 4-1, those four patterns are dense growth of immature films (DGIF), sparse growth of intermediate films (SGIF), sparse growth of intermediate films with ghosting (SGIF-g), and highly interconnected films (HIF).

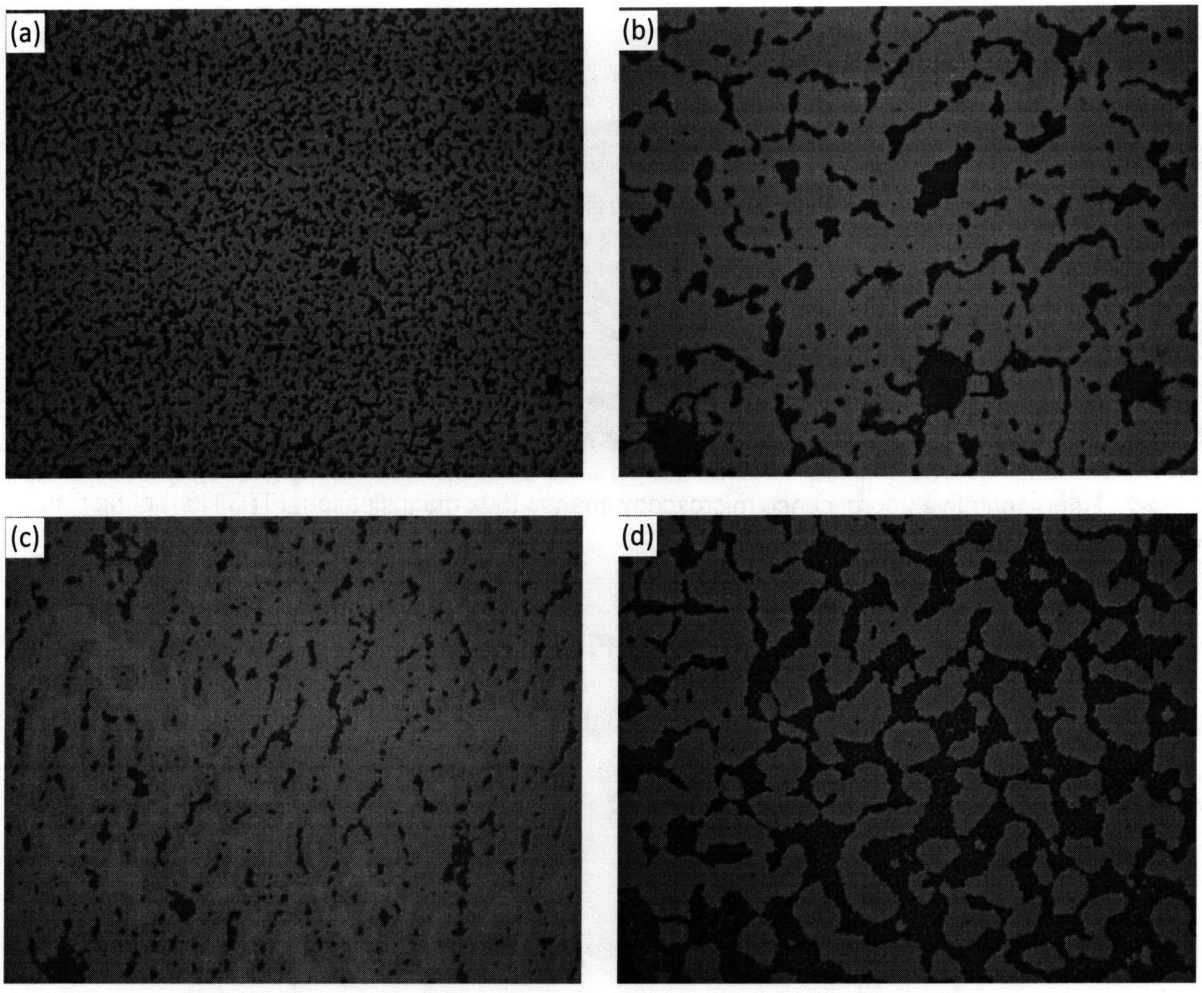

Figure 4-1. Fluorescence microscopy images (50x magnification, FITC filter) representative of (a) DGIF, (b) SGIF, (c) SGIF-g), and (d) HIF biofilm growth patterns.

While all the samples images exhibited more than one of the growth patterns, DGIF growth was only seen on the blank polystyrene substrate and SGIF-g growth was only seen in the two

SPS/PAH systems. Polystyrene has the densest growth of biofilm out of all the systems, and image (a) in Figure 4-1 is largely representative of biofilm growth across the sample substrates. All other samples, which were those with PEM substrates, did not have as many biofilm source points. This lower density of biofilm 'nucleation' sites could result from the biocidal efficacy of the underlying antibacterial PEMs. Given the widespread biofilm growth patterns seen on the PEMs, a correlation between density of biofilm source points and type of PEM substrate could not be established.

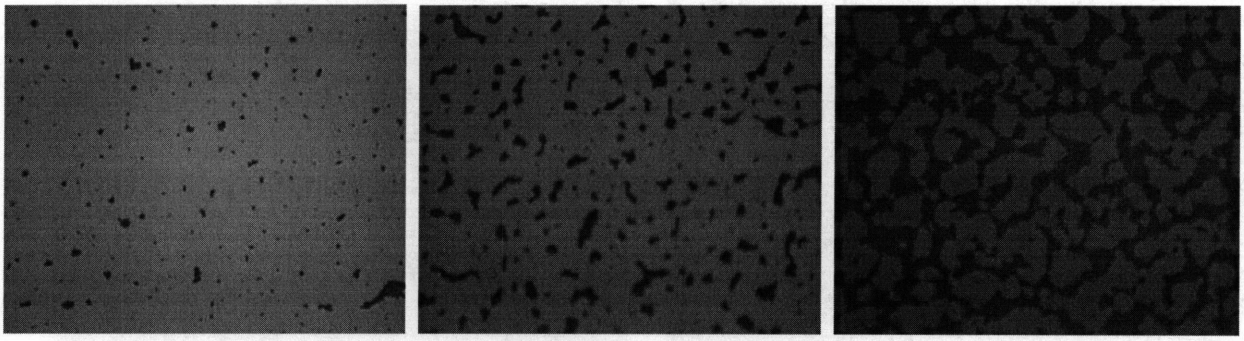

Figure 4-2. Representative fluorescence microscopy images (50x magnification, FITC filter) of biofilms grown on PAA/PAH.

The PAA/PAH samples displayed the DGIF, SGIF, and HIF growth patterns in the 2 hr growth period. Compared to bare polystyrene DGIF growth, PAA/PAH had much less biofilm starting sites. Figure 4-3 illustrates this contrast in density of starting sites.

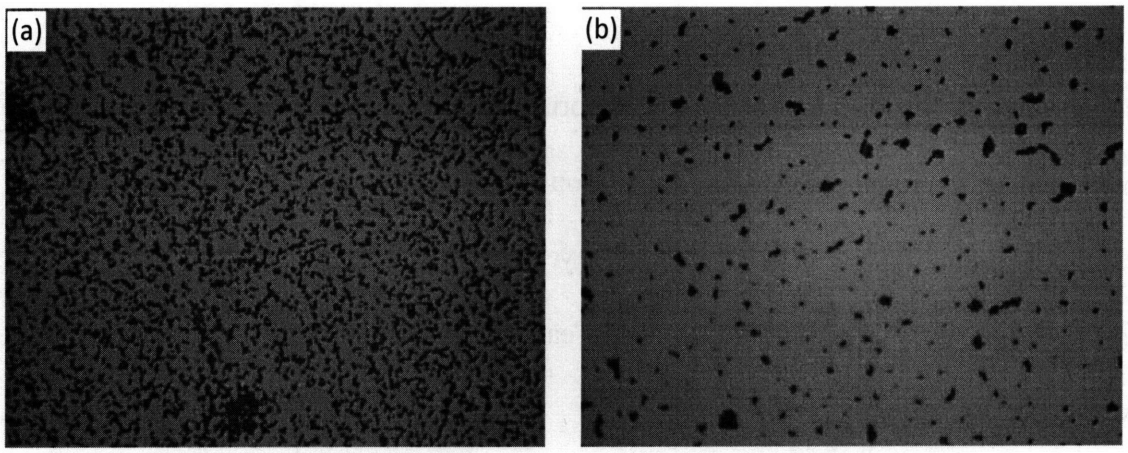

Figure 4-3. Comparison of the DGIF growth patterns on (a) bare polystyrene and (b) PAA/PAH.

The ghosting effect in SGIF-g refers to the dark green shadow-like features that extend from the stained biofilms, seen in Figure 4-4. It is not yet known what this ghosting is composed of, but it is theorized here that the features are remnants, possibly exopolysaccharides, of biofilms that had grown on the substrate but had detached in the process of fixation and/or staining. This theory is based off of the observation that ghosting is only seen extending radially from imaged biofilms and the fact that significant SPS/PAH expansion/shrinking during the wetting and drying procedures could have triggered detachment of biofilm. The extent of this latter concept can be seen in the fragmentation of large biofilms, especially pronounced around the biofilm edges.

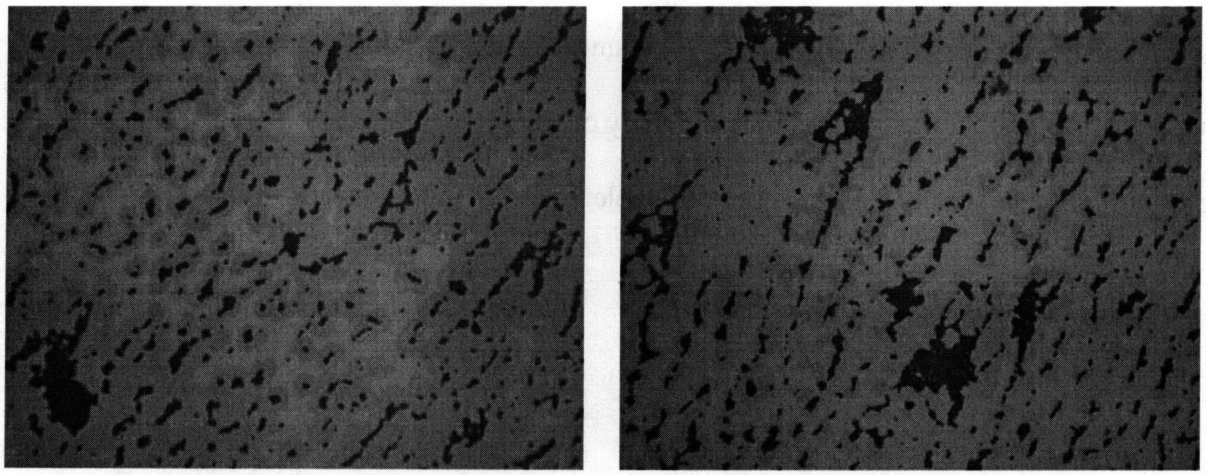

Figure 4-4. Ghosting effects seen as dark green shadows extending from stained biofilms

The most advanced biofilm structures seen are categorized in HIF growth. These biofilms exhibit a high level of interconnectivity, and the reason for these elongated, networked biofilms over, for example, impinging circular biofilms is not yet known. One possible explanation is that quorum sensing between the S. epidermidis biofilms causes expanding biofilms to preferentially expand towards nearby neighbors.

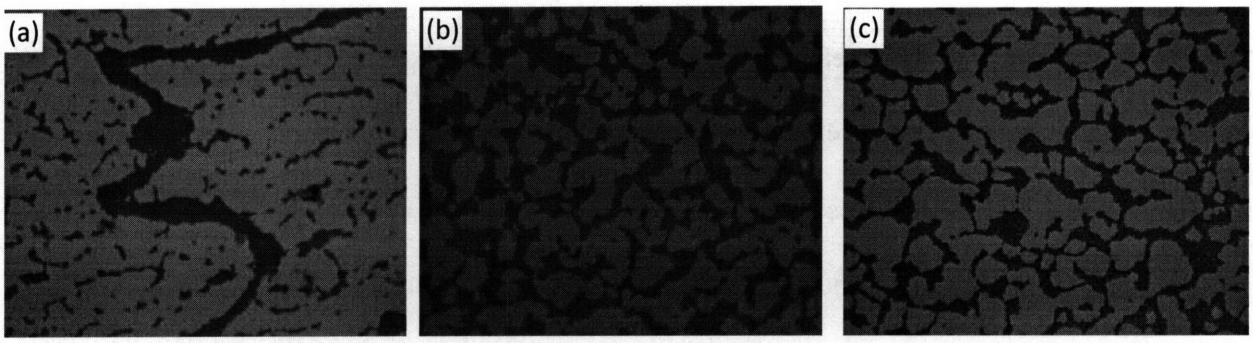

Figure 4-5. HIG growth seen in SPS/PAH acid treated and PAA/PAH substrates. Note the fragmentation of biofilms in (b) SPS/PAH acid treated versus in (c) PAA/PAH.

Several of the SPS/PAH untreated and acid treated substrate samples exhibited recurring artifacts best described as dark, fibrous aggregates. Some examples are show in Figure 4-6. These artifacts were seen via UV microscopy with a FITC filter, but also appear as bright, transparent spots visible microscopy. These artifacts were found in multiple samples of each SPS/PAH untreated and acid treated substrates but not in any of the other substrates. This artifact could be dead cells/biofilms partially stained by crystal violet that fouled the surface.

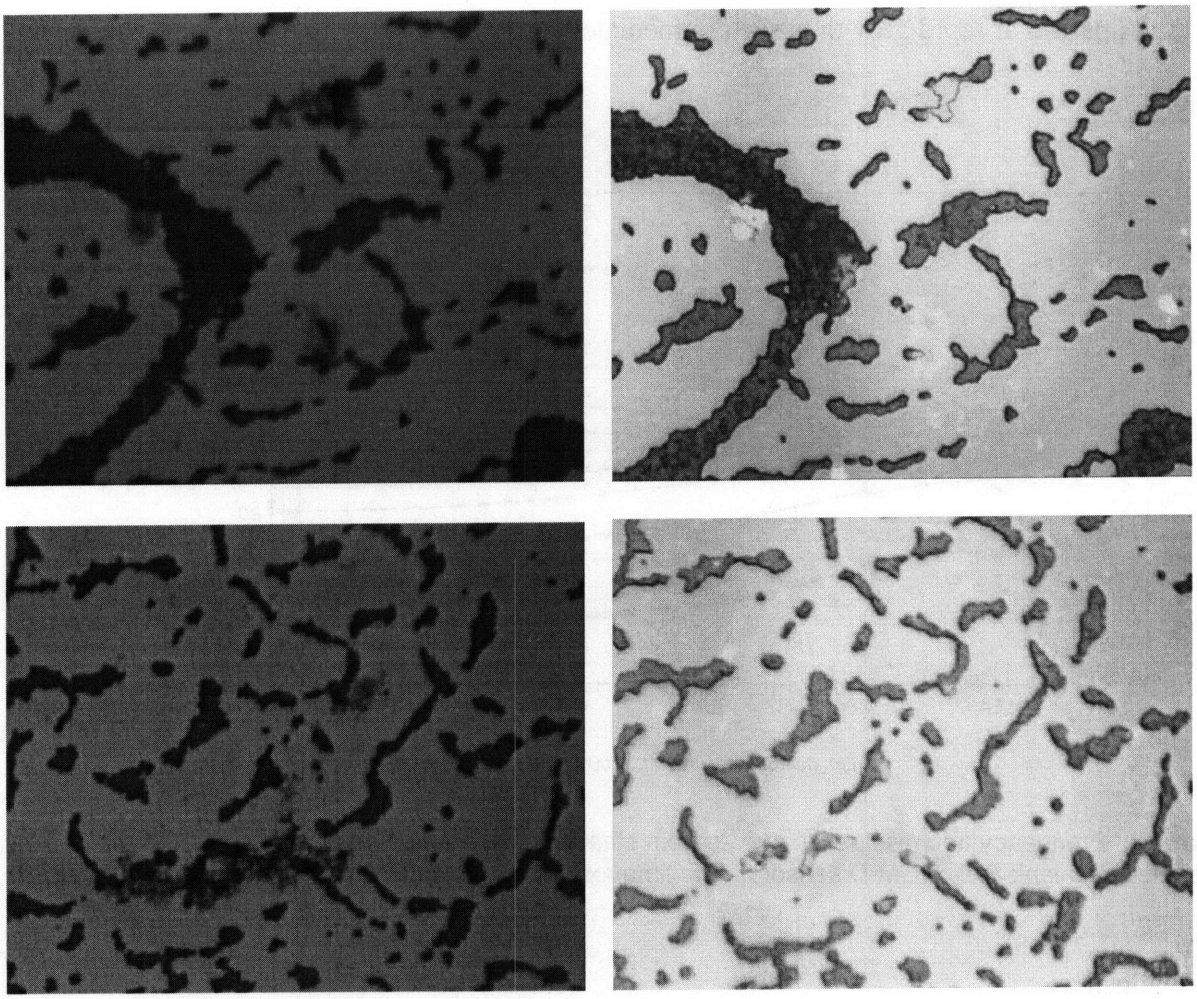

Figure 4-6. Recurring artifacts seen in UV microscopy (left) and in visible microscopy (right).

4.3.2 QCM-D static biofilm growth

S. epidermidis static biofilm growth was successfully tested on QCM-D. Biofilms were grown on blank SiO_2, and the frequency and dissipation curves indicated successful bacteria adhesion onto the QCM-D sensor surface. S. epidermidis suspension was flowed into the QCM-D flow chambers and allowed to sit for 120 minutes at 37°C. This was to allow bacteria fixation and initial biofilm growth. After that, soy trypticase broth was flowed through to support biofilm

growth. A period of rapid growth is seen immediately after the 2 hour adhesion period, seen in Figure 4-7.

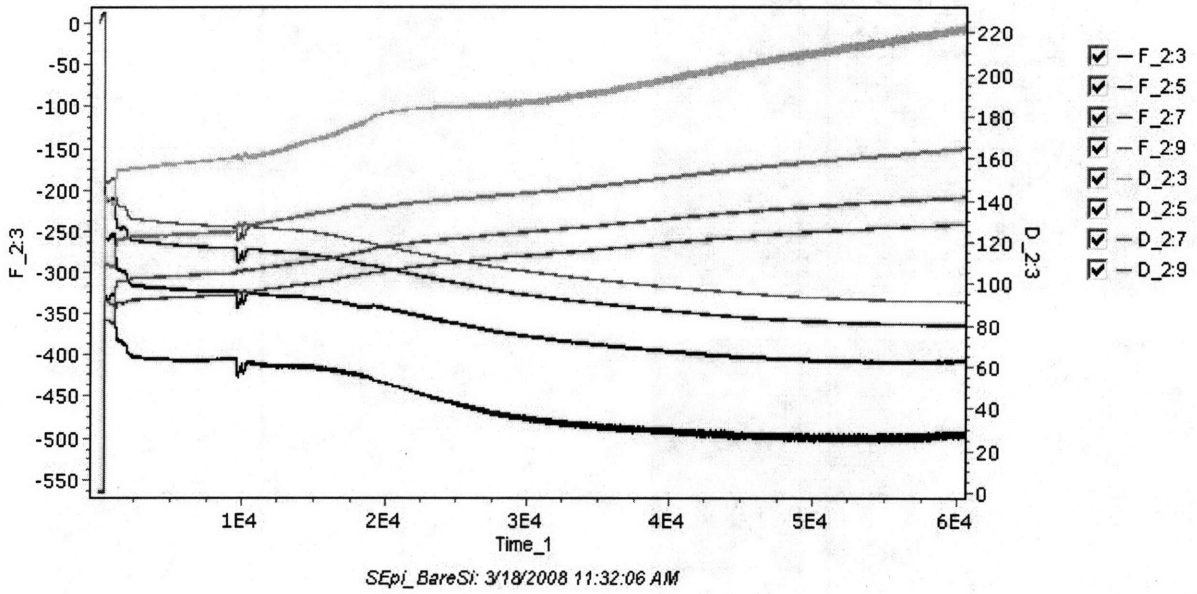

Figure 4-7. Frequency and dissipation curves from static adhesion and subsequent growth of S. epidermidis on blank SiO_2 QCM-D sensors. The time axis covers 0 to 1000 minutes.

4.4 Conclusion

The initial biofilm data provides substantial insight on the qualitative behavior of biofilm growth across the tested substrates. Biofilm growth was categorized into four growth patterns (DGIF, SGIF, SGIF-g, HIF), and multiple patterns were seen in each sample, all of which were incubated for the same time length of 2 hours. All three PEM substrates showed a decrease in the density of biofilm starting sites, although the same conclusion could not be reached for overall biofilm surface coverage. This decrease is likely due to the biocidal effect of the underlying PEM. It is still inconclusive as to whether these antibacterial substrates also slow down or stop biofilm growth. A ghosting effect, characteristic of SGIF-g growth, was also observed in both untreated and acid-treated SPS/PAH substrates. It is postulated here that the

ghosting effect is actually the exopolysaccharide and other structural remnants that remain after biofilm releases from the substrate from repetitive PEM swelling-shrinking. The highly interconnected, advanced biofilm growth seen in HIF regions is observed with a suggested explanation that quorum sensing causes preferential biofilm growth towards neighboring biofilms. Finally, UV/visible microscopy revealed some unexplained artifacts seen as dark fibrous clumps in UV microscopy with a FITC filter and as bright, transparent spots in visible microscopy. Dead bacteria/biofilm may be the cause of these artifacts, but more evidence is needed to identify whether the artifact is a significant property of the biofilm samples.

Initial QCM-D static biofilm growth resulted in the successful growth of S. epidermidis biofilm on bare SiO_2. No further experimentation was done with the grown biofilms, and should be pursued in future work.

REFERENCES FOR CHAPTER 4

1. Mendelsohn, J.D.; Yang, S.Y.; Hiller, J.A.; Hochbaum, A.I.; Rubner, M.F. *Biomacromolecules* **2003**, 4, 96.
2. Thompson, M.T.; Berg, M.C.; Tobias, I.S.; Lichter, J.A.; Rubner, M.F.; Van Vliet, K.J. *Biomacromolecules* **2006**, 7, 1990.
3. Yang, S.Y.; Mendelsohn, J.D.; Rubner, M.F. *Biomacromolecules* **2003**, 4, 987.

CHAPTER 5 SUMMARY AND FUTURE WORK

5.1 Thesis Summary

This research has shown that the antibacterial effect of high density cationic surface charges on PAA/PAH and SPS/PAH PEMs also applies, to a limited extend, to an anti-biofilm effect with gram positive S. epidermidis. Growth on all PEM systems resulted in a lower density of sites of biofilm formation relative to growth on bare polystyrene. This is attributed to a lower survival rate of S. epidermidis on the PEM substrate, leading to fewer occurrences of bacteria density being sufficient to initiate biofilm growth. Given the wide spectrum of biofilm growth and formation on each sample substrate, a general rubric was developed to categorize and describe growth on all tested samples. Surface charge measurements with Rose Bengal and carboxyl-modified microspheres revealed the SPS/PAH acid treated system had the highest density of cationic surface charges while PAA/PAH had the lowest density of cationic surface charges. This could not be correlated to the anti-biofilm effects due to the wide range of biofilm growth patterns exhibited on each PEM system and the inability to conclusively declare one PEM system more anti-biofilm than another. QCM-D was successfully tested for PEM and static biofilm growth, and could potentially provide the basis for a more generalized biofilm growth rubric based on clean versus biofilm-covered ratios and the distribution of young to mature biofilms based on frequency and dissipation measurements.

5.2 Future Directions

This research has identified several promising directions to better examine the biocidal cationic mechanism of action and the behavior of biofilm growth on PEMs.

5.2.1 PEM Growth

The current PEM systems still have a significant amount of characterization needed in relation to biofilm growth. One of the concerns raised during this research was the dipping PEM growth protocol when used with 6-well polystyrene tissue culture plates. Given the geometry of the wells and relatively small surface area, there is increased risk of non-uniform PEM film assembly. These concerns can be addressed through ellipsometry measurements of the PEM thickness built in the tissue culture plates.

5.2.2 Surface charge measurements

As seen from the absorption spectra of the Rose Bengal stained PEMs, it would be wise to reduce stain length to one minute in order to minimize Rose Bengal absorption by the PEM bulk. A more ambitious undertaking would be to model the surface energetics of the carboxyl-modified microspheres to derive the density of free surface amines on PAH. Such modeling could use data from adhesion measurements from prior art conducted by Lichter et al as well as zeta potential measurements to measure the charge of the microspheres. The calculations of the surface charge densities could reveal significant trends in anti-biofilm behavior, such as threshold surface charge densities for both theorized mechanisms of cell kill. Quantified surface charge density also enables incorporation of other systems factors, including charges associated

with the bacteria and charges derived from the solution pH. Another important test may be zeta potential measurements of PEMs built on microparticles. The zeta potential of the outermost layer could be probed at each adsorption step and after acid treatment.

5.2.3 Future biofilm work

Biofilm growth. In pursuing the biofilm studies with microscopy, further work needs to be conducted in understanding the growth and behavior of S. epidermidis on ideal substrates. Doing so establishes a baseline or control for comparison with the PEM substrates. This can be achieved by growing biofilms on bare polystyrene and glass substrates. The 'growth on polystyrene' biofilm growth protocol can be used for each substrate, and with multiple samples made for each substrate. These batches of identical substrates, grown under identical conditions, will be given varying biofilm growth times by fixating and staining samples at regular intervals (30 to 60 minutes). Extremely special care should be taken during the fixation and staining protocols to ensure that biofilm is not being removed, loosened, or modified during the process. The result is a series of samples that can be imaged to show biofilm growth over time on control substrates. The images from these samples will characterize expected S. epidermidis biofilm growth and will enable further comparative analysis with the PEM substrate biofilms.

Biofilm imaging. One of the difficulties encountered in this biofilm study was the lack of a robust rubric for grading biofilm growth. The crystal violet stains had the negative effects staining the PEM substrate and providing limited data in terms of visible biofilm structure. A

study by Donlan and Costerton suggests a few methods that could improve biofilm measurements. Electron microscopy has been used frequently in the past, but required modification and alteration of biofilm samples. On the other hand, confocal laser scanning microscopy (CLSM) delivers 3-D spatial information while keeping the biofilm unaltered and intact. Structure can also be used to grade biofilm maturity. For example, specific polysaccharide stains like ruthenium red can be used to image the exopolysaccharide matrix that is characteristic of biofilms. The bacteria within the structure can also be target via fluorescent nucleic acid stains such as DAPI, acridine orange, and Syto 9. These stains can even selectively stain cells based on various properties. For example, propidium iodide is only taken up by cells with damaged cytoplasmic membranes. Combine with 5-cyano-2,3-ditolyl tetrazolium chloride, which is reduced to 5-cayno-2,3-ditolyl tetrazolium chloride-formazan if the stained cells have functioning cytochrome system, to measure the ratio of intact versus broken cells. Given that the studied antibacterial mechanism of action relies on membrane puncture of some degree, this test could prove useful beyond just biofilms to clarify the requirements for the polycationic biocidal effect. [2]

Biofilm quantification. Another method of grading biofilm growth is to remove the fixation step of the biofilm protocol and instead release the biofilm from sample substrates, re-suspend bacteria cells, and culture. The prevalence of bacterial colonies for each sample will indicate success of biofilm growth, but significant data, including biofilm structure, bacteria cell differentiation, and biofouling of PEM surface is lost.

Additional biofilms of interest. Study of the current systems under flow conditions would enable a greater understanding of how biofilms grow in dynamic and physiological environments. Such continuous biofilm growth has been successfully conducted with flow chambers and using QCM-D.[1,3,4] Also of interest is expansion of the biofilm studies to include gram negative bacteria. Biofilm forming E. coli would be the first choice, given its extensive study and thorough understanding of the organism. Other significant biofilm-forming bacteria to study, based on general level of interest and prior characterization, include S. aureus and P. aeruginosa.

REFERENCES FOR CHAPTER 5

[1] Christensen, B.B.; Sternberg, C.; Andersen, J.B.; Palmer, R.J.; Nielsen, A.T.; Givskov, M.; Molin, S. *Methods in Enzymology* **1999**, 310, 20.

[2] Donlan, R.M.; Costerton, J.W. *Clinical Microbiology Reviews* **2002**, 15, 167.

[3] Klausen, M.; Heydorn, A.; Ragas, P; Lambertsen, L.; Aaes-Jorgensen, A.; Molin, S.; Tolker-Nielsen, T. *Molecular Microbiology* **2003**, 48, 1511.

[4] Schofield, A.L.; Rudd, T.R.; Martin, D.S.; Fernig, D.G.; Edwards, C. *Biosensors and Bioelectronics* **2007**, 23, 407.